BIOCHEMISTRY
including biophysical chemistry & molecular biology

Article

pubs.acs.org/biochemistry

Effect of Loop Composition on the Stability and Folding Kinetics of RNA Hairpins with Large Loops

Artem V. Melnykov,[†,§] Rajesh K. Nayak,[‡,§,∥] Kathleen B. Hall,*[,†] and Alan Van Orden*[,‡]

[†]Department of Biochemistry and Molecular Biophysics, Washington University School of Medicine, St. Louis, Missouri 63110, United States

[‡]Department of Chemistry, Colorado State University, Fort Collins, Colorado 80523, United States

Supporting Information

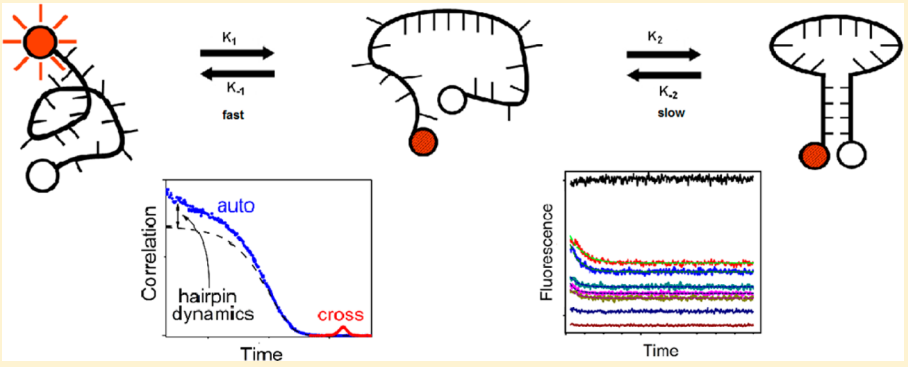

ABSTRACT: RNA hairpins are ubiquitous structural elements in biological RNAs, where they have the potential to regulate RNA folding and interactions with other molecules. There are established methods for predicting the thermodynamic stability of an RNA hairpin, but there are still relatively few detailed examinations of the kinetics of folding. Nonetheless, several recent studies indicate that hairpin folding does not proceed via a simple two-state model. Here, we monitor fluorescence from hairpins constructed as molecular beacons in ensemble, fluorescence correlation spectroscopy, and stopped-flow experiments to describe the folding of RNA hairpins with long (15 nucleotide) loops. Our results show that folding of these hairpins occurs through more than two states and that the mechanism of folding includes a fast intermediate phase observed on the tens of microseconds time scale and a slow phase, attributed to formation of the native folded hairpin loop and stem, observed on the milliseconds time scale. The composition of the RNA loop determines the time scale of intermediate and native folded states. Hairpins with a polyuracil loop sequence exhibit slower relaxation of the intermediate state and faster relaxation of the native folded state when compared to that of hairpins with cytosine or adenine in the loop. We hypothesize this composition dependence could be attributed to nucleobase stacking in cytosine and adenine containing regions of the loop, which would be absent in hairpins containing polyuracil loops. Such base stacking could destabilize the intermediate folds, thereby speeding the relaxation of the intermediate relative to similar sized hairpins with no base stacking in the loop. Likewise, the lower intermediate stability could prolong the relaxation of the native folded state.

Hairpins are secondary structure elements in RNA molecules, formed by the nucleic acid folding on itself to make a loop ending with a double helical region (stem). RNA hairpins serve a great variety of functions either as independent structural elements or as participants in tertiary interactions.[1] Once a hairpin has been formed, the ensemble of possible secondary structures is constrained, so a hairpin can serve as a selector between alternative RNA folds. Therefore, it is important to understand dynamic as well as equilibrium properties of RNA hairpins. On the mechanistic level, this means knowing the nature of the folded, unfolded, and partially folded states as well as the free energy barriers that separate these states. There are many challenges to describing these states, which are dependent on the sequence and length of the loop, the stability of the stem, and alternative structures of the RNA, and, consequently, the folding free energy landscape of an RNA hairpin has been described as rugged.[2−6]

Traditionally, thermodynamics of RNA hairpins is understood in terms of a reductionist model.[7,8] The stability of the stem is predicted according to the nearest-neighbor interaction model while the loop contributes a destabilizing free energy (an empirical factor for loops shorter than 10 nucleotides, with the notable exception of ultrastable tetraloops). The assumptions associated with this model are that (i) there are no interactions between the loop and the stem, (ii) the nearest neighbor model is accurate, and (iii) sequence specific effects and interactions

Received: November 18, 2014
Revised: January 26, 2015
Published: February 20, 2015

DOI: 10.1021/bi5014276
Biochemistry 2015, 54, 1886−1896

within the loop can be neglected. Despite these assumptions, the model is a successful predictor of thermodynamic stability of many RNA hairpins.

Kinetics of RNA and analogous DNA hairpin folding has, in the past, been interpreted using a two-state model,[9,10] folded ↔ unfolded, which can be understood in simple terms if the initial encounter of the 5′ and 3′ termini of the RNA strand is followed by a rapid zippering to form the stem. In the case of RNA hairpins, several theoretical studies[11−17] have challenged the two-state model, suggesting that alternative secondary structures can be important as intermediates even in rather short RNA hairpins. Theoretical developments were further spurred by observation of two or more relaxation phases in several nucleic acid hairpins after a temperature jump near the melting temperature.[2,3,18] In the case of DNA hairpins, evidence for multiple states and intermediates in the folding mechanism has been obtained from recent investigations using fluorescence correlation spectroscopy,[19−22] stopped-flow kinetics,[23] and stopped-flow kinetics combined with temperature jump.[24]

Base stacking is present in single strands of both DNA and RNA.[25] Different sequences have different stacking propensities, with polyuracil showing no stacking interactions and both polyadenine and polycytosine having stacking interactions with large enthalpies. When these nucleotides are present in the loop of a potential hairpin, the effect of their stacking properties on hairpin folding is not clear. Experimental data suggest that, at least in a short tetraloop with a two base pair stem, stacking interactions can be responsible for folding intermediates.[2] While the role of base stacking in the loop on the kinetics of larger DNA hairpins has been investigated previously,[26−30] to our knowledge, a theory that explicitly accounts for single-stranded base stacking in hairpin folding has not yet been achieved.

To further investigate the effect of loop sequence on RNA folding kinetics, we studied the thermodynamic stability and folding kinetics of three RNA hairpins with identical four base pair stems but different 15 nucleotide loop sequences. The three loop sequences investigated consisted of polyuracil, polypyridine with alternating uracil and cytosine repeats, and the same polypyrimidine sequence with one of the cytosines replaced with adenine. These sequences are thought to vary in their propensity for base stacking in the loop region and their ability to form non-native base pairing contacts. In particular, the latter two sequences are believed to exhibit a propensity for base stacking in the loop due to the presence of cytosine and cytosine−adenine containing repeats, whereas the polyuracil loop should have no propensity for base stacking. Additionally, the hairpin with the adenine substitution in the loop exhibits a more diverse ensemble of secondary structures compared to that of the two polyuracil and polypyrimidine containing hairpins (see Supporting Information Figures S1 and S2). Hence, the role of these factors on the hairpin folding kinetics can be explored.

To enable high-sensitivity detection of folding events, the hairpins were labeled with a fluorophore on the 3′ end and a quencher on the 5′ end. This detection scheme (a "molecular beacon") is very sensitive[31] and has been used to study folding of DNA hairpins.[10,19,20,22,23,27] We employed steady-state absorption and fluorescence spectroscopy to elucidate equilibrium properties of the labeled RNA hairpins and fluorescence correlation spectroscopy (FCS) and stopped-flow kinetics to study folding dynamics.

FCS is a technique that allows measurement of relaxation rates of chemical reactions at equilibrium.[32] When reactants are characterized by different molecular brightness, it is possible to analyze the fluorescence autocorrelation function and obtain rate constants from its decay. In the hairpins studied here, there are several conformational changes that are accompanied by quenching and may be reflected in the correlation functions. According to the labeling scheme used, formation of a partially or fully folded stem brings the dye and the quencher in close proximity, resulting in nearly complete quenching of the dye. However, conformations of the hairpin with a frayed stem may not all be quenched to the same extent and hence separation of the ends without complete disruption of the stem may also be detected as an isomerization process. In addition, fluorescence may be quenched as a result of random encounter of the dye with the quencher or a nucleobase, and this process can be affected by non-native secondary structure formation. In the following sections, we refer to all mentioned transitions among dark and bright conformations as isomerization and develop molecular interpretation of the observed transitions throughout.

Since FCS experiments are carried out in solution, diffusion of the molecules is always reflected in the autocorrelation curve as a competing relaxation process. Therefore, from the practical point of view, it can be hard to reliably measure both relaxation rates, especially when they happen on the same time scale. Two-beam flow FCS[33] was designed to alleviate this problem by introducing a second probe beam and aligning the two observation regions with the sample flow. The width of the cross-correlation peak calculated from the two beams serves as an independent measure of the diffusion coefficient and hence relaxation due to isomerization can be measured more reliably. Because of the limitations of our FCS experiment, we can measure relaxation times between 1 and ∼250 μs; we refer to processes that happen in this time window as the fast phase. Slower isomerization is reflected in FCS data indirectly (through a change in the apparent number of fluorescent molecules in the optical probe region), and we call this the slow phase. This slow phase can be directly monitored by stopped flow. This same strategy was employed previously to monitor similar fast and slow phase isomerization reactions in DNA hairpins.[20,23]

We first show that thermodynamic parameters of RNA hairpin folding are somewhat probe-dependent, which suggests possible deviations from a strictly two-state mechanism. Next, we describe results of FCS experiments that also indicate a more complex folding scheme and, in addition, show that folding dynamics is influenced by the nucleobase sequence in the loop. For a small population of molecules, we observe isomerization on the submillisecond time scale. Stopped-flow measurements reveal the slow phase of the reactions on time scales >500 μs. Our results emphasize again that RNA hairpin folding is not two-state and provide a new interpretation of the intermediates.

METHODS

Experiments were carried out in 2.5 mM sodium-cacodylate buffer (pH 7.4) containing 250 μM EDTA and varying KCl concentration (0−500 mM). All solutions were filtered through 0.45 μm Nalgene nitrocellulose filter units to remove any contaminating proteins.

RNA Hairpins and Control Samples. We designed three RNA hairpins that have identical stems but different loop

DOI: 10.1021/bi5014276
Biochemistry 2015, 54, 1886−1896

sequences. These sequences are given as follows, with the stem portion underlined: (i) polyU loop hairpin (hpU) 5′-CGGUUUUUUUUUUUUUUGCCG-3′, (ii) polypyrimidine loop hairpin (hpPy) 5′-CGGUUUCCCUCCCUCCUUUGCCG-3′, and (iii) polypyrimidine loop hairpin with a single adenine (hpPyA) 5′-CGGUUUCCCUCCCACCUUUGCCG-3′. Note the stems consist of three Watson−Crick base pairs and one wobble GU pair. In order to enable high-sensitivity detection of hairpin closing, all three RNA constructs are labeled with a fluorophore (5-TAMRA) on the 3′ end and a quencher (dabcyl) on the 5′ end. We call these constructs hpU-QF, hpPy-QF, and hpPyA-QF, respectively. Quenching of TAMRA by dabcyl is very efficient (99%) but is not understood at the molecular level; the contribution of FRET is negligible with spectral overlap being only 0.15.[31]

Control sequences for the experiments include: polyU loop hairpin without the quencher on the 5′ end (hpU-F), single-stranded (not a hairpin) RNA consisting of 23 uracils labeled with both dabcyl and TAMRA (ssU-QF), and single-stranded DNA with the sequence 5′-TTTTTTTTTTTTTTTTTTTTTTTG-3′ labeled with TAMRA on the 3′ end (ssTGdna-F). All nucleic acid samples used in this study were purchased from IBA GmbH, Germany.

Absorption Measurements. Absorption spectra were recorded on a Shimadzu UV-1800 spectrophotometer equipped with a thermoelectrically temperature-controlled cell holder. Melting experiments were performed on a Gilford 260 spectrophotometer equipped with a 2527 Gilford thermoprogrammer. Sample solutions contained 3 μM RNA in buffer. All samples were heated at 90 °C and cooled to the starting temperature of the melt to eliminate air bubbles. The samples were then heated at the rate of 1 °C/min while monitoring absorbance at either 260 or 554 nm. All temperature unfolding experiments were analyzed in terms of a two-state model with independent linear baselines for both states.

Fluorescence Measurements. Measurements of excitation spectra and fluorescence melts were carried out on an SLM-8100 spectrofluorometer equipped with a water bath for sample temperature control. Sample solutions contained 50 nM RNA in buffer and varying amounts of KCl. Excitation spectra were recorded by monitoring fluorescence at 610 nm (4 nm excitation bandwidth, 16 nm emission bandwidth), whereas melting curves were obtained by excitation at 555 nm and observation at 585 nm (4 nm excitation and emission bandwidths). All measurements were performed with polarizers set at the magic angle to avoid polarization-dependent effects.

Stopped-Flow Measurements. Stopped-flow measurements were used to observe the slow phase isomerization of the hairpins after a mixing time of 450 μs. Measurements were carried out using an Applied Photophysics SX-20 instrument (Surrey, United Kingdom). Sample solutions containing 70 nM RNA hairpins in buffer were mixed with buffer solutions containing varying concentrations of KCl in a 5 μL mixing cell. Folding reactions were monitored by observing the quenching of the TAMRA dye after the mixing time. The dye fluorescence was excited at 547 nm (2 nm bandwidth) and observed through a 570 nm high pass filter. Control samples consisting of TAMRA-labeled RNA hairpins with no quencher, and blank buffer solutions were also measured for comparison.

Dual-Beam FCS. Dual-beam FCS was used to measure the fast phase isomerization of the hairpins on the 1−500 μs time window. The instrument for dual-beam FCS (described in detail elsewhere[19,20,33]) was modified for TAMRA excitation and observation. A 532 nm laser (Edmund Optics, NJ) was used for excitation, while the emission path was modified with a 532 nm dichroic beam splitter (Zeiss, Germany) and HQ550LP emission filter (Chroma Technology, VT). Raw photon records from both channels were stored on a personal computer interfaced with a FLEX card (http://correlator.com, FLEX01-12D). An in-house C program was used to calculate auto- and cross-correlation functions with the desired number of points and time resolution. The fitting range of the autocorrelation curves was constrained to the time delay exceeding 1 μs because of the strong presence of afterpulsing for shorter time lags.

All FCS measurements were carried out in cleaned glass capillaries coated with poly(vinyl alcohol) as described previously.[33] Sample solutions contained 50 nM RNA in buffer and KCl. The samples were injected into the capillaries from glass vials treated with Sigmacote (Sigma, MO). This capillary and sample vial treatment ensures reproducible and constant count rates throughout the measurement.

Data Analysis. A calibration experiment with a control sample (ssTGdna-F) allowed us to estimate separation between the beams. Solutions of 10 nM ssTGdna-F in 20 mM KCl buffer were studied with and without flow. The experiment in the absence of flow measured the diffusion time of the DNA molecules by fitting the decay of the autocorrelation curve to eq 1

$$g_{A,A}(\tau) = \frac{1}{N_{A,A}} \frac{1 - f + f\, e^{-\tau/\tau_{tr}}}{1 - f} \left(1 + \frac{\tau}{\tau_D}\right)^{-1} \quad (1)$$

where $N_{A,A}$ is the apparent number of molecules in the beam, τ_D is the diffusion time of the molecules, and f and τ_{tr} are the amplitude and the relaxation time of the triplet state, respectively. The obtained diffusion time was then used to analyze the cross-correlation obtained in the presence of flow. The fitting equation

$$g_{A,B}(\tau) = \frac{1}{N_{A,B}} \left(1 + \frac{\tau}{\tau_D}\right)^{-1} \exp\left[-\frac{\left(1 - \frac{\tau}{\tau_F}\right)^2 r^2}{1 + \frac{\tau}{\tau_D}}\right] \quad (2)$$

has three free parameters: $N_{A,B}$, the number of molecules as determined by cross-correlation; τ_F, the flow time (the amount of time it takes on average for a molecule to travel between the beams); and r, the separation between the beams relative to the size of the beam. The last parameter is a property of the system and, once determined, was fixed for the rest of the measurements. For the majority of the experiments reported here, r = 15, which was sufficient to prevent cross-talk between the two beams. In addition, the triplet state parameters obtained in this experiment were fixed in subsequent data analysis.

FCS data from other control and hairpin samples were collected at different KCl concentrations. One FCS experiment consists of auto- and cross-correlation functions averaged over ten 1 min measurements. Such data set is analyzed globally so that the autocorrelation ($g_{A,A}$) and the cross-correlation ($g_{A,B}$) are fit simultaneously. This procedure makes full use of diffusion information that is contained in both auto- and cross-correlations. The data were fit to a model with a triplet state and an isomerization reaction

DOI: 10.1021/bi5014276
Biochemistry 2015, 54, 1886−1896

$$g_{A,A}(\tau) = \frac{1}{N_{A,A}} \frac{1 - B + B\, e^{-\tau/\tau_{iso}}}{1 - B} \times \frac{1 - f + f\, e^{-\tau/\tau_{tr}}}{1 - f} \left(1 + \frac{\tau}{\tau_D}\right)^{-1} \exp\left[-\frac{\left(r\frac{\tau}{\tau_F}\right)^2}{1 + \frac{\tau}{\tau_D}}\right] \quad (3)$$

$$g_{A,B}(\tau) = \frac{1}{N_{A,B}} \frac{1 - B + B\, e^{-\tau/\tau_{iso}}}{1 - B} \left(1 + \frac{\tau}{\tau_D}\right)^{-1} \exp\left[-\frac{\left(1 - \frac{\tau}{\tau_F}\right)^2 r^2}{1 + \frac{\tau}{\tau_D}}\right] \quad (4)$$

where B and τ_{iso} are the amplitude and the relaxation time of the isomerization process (parameters f, τ_{tr}, and r are fixed in this fit). All parameter values reported in this article are averaged over 5−7 FCS experiments, and the errors are standard deviations of the mean. All fitting parameters are tabulated in Supporting Information Tables S1−S5.

RESULTS

The RNA sequences investigated in this study were designed to determine if loop composition had any effect on hairpin folding. These 15 nucleotide loops are longer than most naturally occurring RNA hairpin loops, which could be advantageous for detection of sequence dependence. As with all RNA strands, these sequences are capable of forming alternative structures, which we enumerated in connectivity files of possible secondary structures and visualized using the UNAfold package.[34] The first of these hairpins, hpU, was shown to form few non-native basepairs, as did hpPy (Figure S1a). The last construct, hpPyA, has many more alternative structures (Figure S1b). The potential for the presence of an ensemble of states must be considered in the interpretation of our data, although the stability of many of the possible folds is very low and they are not expected to be highly populated.

Equilibrium Thermodynamics. The first question we shall address is how the sequence of the loop affects stability of the designed hairpins. The standard way to determine equilibrium thermodynamic parameters of a hairpin is to perform a thermal melting experiment while monitoring the transition to the unfolded structure by measuring absorbance at 260 nm. Since these hairpins are labeled, TAMRA fluorescence can also report on stem melting. Finally, it is known[31] that the absorption spectrum of TAMRA is affected by proximity to the quencher, so its absorbance also reports on the transition.

The temperature dependence of TAMRA absorption in the context of hpU-QF is shown in Figure 1, where the changes observed in the spectra are very similar to what was previously reported for molecular beacons.[31] The presence of an isosbestic point (509 nm) indicates that there are two populations of RNA structures in solution in this temperature range. There is no change in the shape of the excitation spectrum of the hairpin for a wide range of salt concentrations (0−500 mM KCl) at 45 °C, whereas the fluorescence intensity changes more than 10-fold (Figure S2). The melting temperature of the hairpin varies between 25 and 60 °C across this range (Figure S4) so that the hairpin is unfolded at 0 mM and folded at 500 mM KCl.

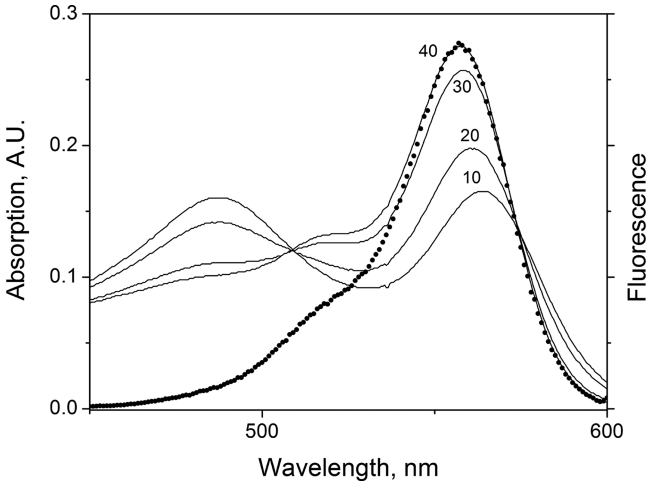

Figure 1. Absorption and excitation properties of 2 μM hpU-QF in 0 mM KCl buffer (2.5 mM sodium cacodylate, pH 7.4, 250 μM EDTA). Four absorption spectra of the hairpin for 10, 20, 30, and 40 °C are shown (lines). The excitation spectrum recorded at 40 °C is shown in black circles.

Therefore, we conclude that the excitation spectrum of the hairpin is not affected by its folding state.

Thermal denaturation profiles of hpU-QF depend on the monitored probe. The results of the melting experiments are summarized in Table 1, and examples of raw data are presented in Figure S3. The trends are identical for all three hairpins: the melting temperature depends on the spectroscopic signal used to monitor melting, whereas the enthalpy of transition remains unaffected (within error). The difference between T_m (A_{260}) and T_m (A_{554}) is small (approximately 2 °C) but nevertheless exceeds experimental error in all cases, whereas the melting temperature determined by fluorescence is substantially (5 °C) lower. The dependence of the melting temperature on the spectroscopic signal used to monitor the unfolding transition suggests that hairpin unfolding is not a two-state process. Since the melting temperature determined by TAMRA fluorescence and 554 nm absorption is different, these experiments are likely reporting on two different events or different states of the RNA. The absorbance spectra (Figure 1) show that two states are present during the unfolding process, but other state(s) with different spectral properties may also be present. Similar results were obtained by Xu et al.[35] by monitoring absorption and fluorescence of 2-aminopurine in the stem of a hairpin, and structural conclusions were drawn based on the known properties of the probe. Unfortunately, there is insufficient information about spectral properties of the dabcyl−TAMRA complex, so we are unable to provide structural interpretation of our results.

The three hairpins have similar melting temperatures and enthalpies, as reported by the same spectroscopic probe (Table 1). This result was further tested by melting experiments with fluorescence detection at several salt concentrations. In all cases, the difference in the melting temperature among the three hairpins was not significant (Figure S4). While stacking in the loop is known to lower the melting temperature,[27,28] we did not observe this effect in the hairpins studied.

Kinetic Measurements by FCS and Stopped Flow. Analysis of hairpin folding by two-beam flow FCS provides access to submillisecond isomerization rates at equilibrium. An example of data from the two-beam experiment is shown in

DOI: 10.1021/bi5014276
Biochemistry 2015, 54, 1886−1896

Table 1. Thermodynamic Parameters of Hairpin Folding in a Buffer with 100 mM KCl[a]

	T_m, °C						ΔH, kcal/mol					
hairpin	A_{260}		A_{554}		fluor.		A_{260}		A_{554}		fluor.	
hpU-QF	58.6	+1.4	55.4	+0.4	49.9	+0.5	−45.3	+7.3	−42.8	+2.3	−43.3	+2.3
		−1.4		−0.4		−0.6		−8.5		−2.5		−2.4
hpPy-QF	56.3	+0.8	55.0	+0.3	50.9	+0.6	−44.9	+5.1	−42.0	+2.2	−41.2	+2.1
		−0.8		−0.3		−0.6		−5.8		−1.6		−2.2
hpPyA-QF	56.1	+1.0	54.4	+0.4	49.4	+0.6	−37.8	+4.6	−37.9	+1.7	−38.2	+1.9
		−1.0		−0.4		−0.5		−5.2		−1.8		−1.9

[a]Absorbance (260 and 554 nm) and fluorescence experiments were used to monitor the transition. Enthalpy was calculated from fitting the unfolding curves to a two-state model with linear baselines.

Figure 2, where autocorrelation functions obtained with hpU-QF samples are plotted for several salt concentrations (0, 20, 100, and 500 mM) and the corresponding cross-correlation functions are shown in the lower panel on the same time scale. Global analysis of auto- and cross-correlations extracts the contribution of diffusion and flow to the autocorrelation functions; these contributions were calculated and plotted as dashed lines in Figure 2. In the absence of other processes, the calculated and measured autocorrelations should be identical, but for these hairpins, there are clear differences. We propose that the experimental data includes contributions from triplet state formation of the fluorophore (≈4 μs) and hairpin isomerization (20−200 μs).

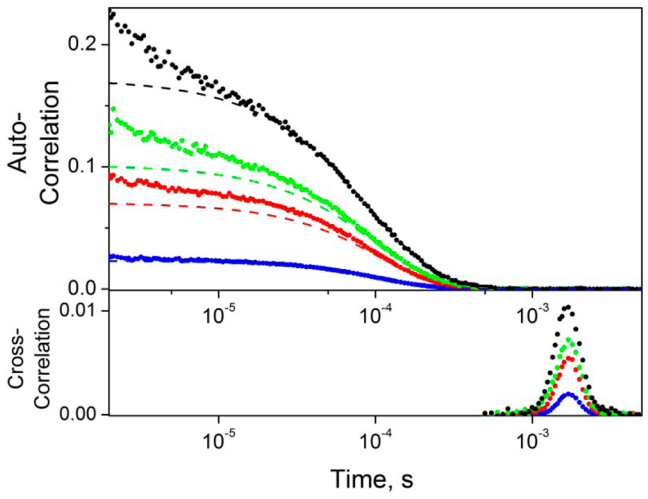

Figure 2. Autocorrelation functions (upper panel) measured from flowing 40 nM hpU-QF solution at different KCl concentrations are plotted in circles (blue, 0 mM; red, 20 mM; green, 100 mM; black, 500 mM KCl) with corresponding cross-correlations shown in the lower panel. The dashed curves are autocorrelation decays due to diffusion and flow only.

Several features of the hpU-QF hairpin can be deduced by close inspection of the correlation data. The amplitude of the cross-correlation (Figure 2, lower panel) is higher for higher salt concentrations, indicating that the number of fluorescent molecules in the optical probe region is reduced. The results of control experiments discussed in the next section give us confidence that the hairpin molecules are still present in solution but are undetectable since they are quenched. These molecules must be characterized by a slow isomerization rate: they adopt conformations that do not relax on the submillisecond time scale of the FCS experiment. Therefore, we observe, although indirectly, a slow phase in hairpin isomerization. At the same time, we directly measure a fast isomerization reaction through the decay of the autocorrelations on the 20−200 μs time scale (Figure 2, upper panel).

The slow phase evident in the FCS data can be observed directly using stopped-flow mixing, in which RNA hairpins in solutions of low ionic strength are mixed with solutions containing different concentrations of KCl to induce folding. Figure 3 shows the stopped flow mixing data for hpU-QF (Figure 3a), hpPyA-QF (Figure 3b), and hpPy-QF (Figure 3c) RNA hairpins. Mixing with KCl induced formation of the folded native RNA hairpins, which could be monitored by observing the quenching of the TAMRA dye as a function of time. Control samples containing only the blank buffer are also shown for comparison. A slow reaction phase >1 ms is clearly evident for all RNA hairpin samples at the lower KCl concentrations. The relaxation time decreases with increasing salt concentration such that the slow phase is no longer evident for the hpU-QF hairpin for KCl concentrations above 50 mM. However, for the hpPy-QF and hpPyA-QF hairpins, slow folding can be observed for KCl concentrations up to 100 mM. Due to the limitations of our FCS and stopped-flow experiments, there is a time window between ∼250 and 500 μs that is inaccessible to both experiments. For hpU-QF isomerization in KCl above 50 mM and hpPy-QF and hpPyA-QF in KCl above 100 mM, it appears that the slow phase of the reaction occurs within this inaccessible time window.

Our FCS and stopped-flow kinetics observations are sufficient to show that folding in these RNA hairpins is not a two-state process. Rather, there is a small population of molecules that undergo fast isomerization on a submillisecond time scale, whereas, at the same time, there is a substantial population of molecules with slower dynamics on time scales >1 ms. Hence, at least three states are necessary to describe the data.

Hairpin Kinetics in the Presence of KCl for Different Loop Sequences. A more quantitative analysis of FCS and stopped-flow data from several RNA hairpins collected at several KCl concentrations reveals the effect of loop composition on hairpin folding. We begin with a discussion of the FCS data. As evidenced by the reduction in the number of molecules with salt concentration probed by FCS (Figure 4a), the slow phase is present in all hairpins, regardless of the loop composition; molecular brightness is similar in all cases (Figure 4b). However, parameters of the fast phase (observed directly in the autocorrelation functions) are different. While the hpU-QF displays a fast decay with a maximum of 200 μs at 10 mM KCl (Figure 4d), the decay rates for hpPy-QF and hpPyA-QF are more rapid. The loop sequences of hpPy and hpPyA contain clusters of uracils and cytosines, in contrast to

DOI: 10.1021/bi5014276
Biochemistry 2015, 54, 1886−1896

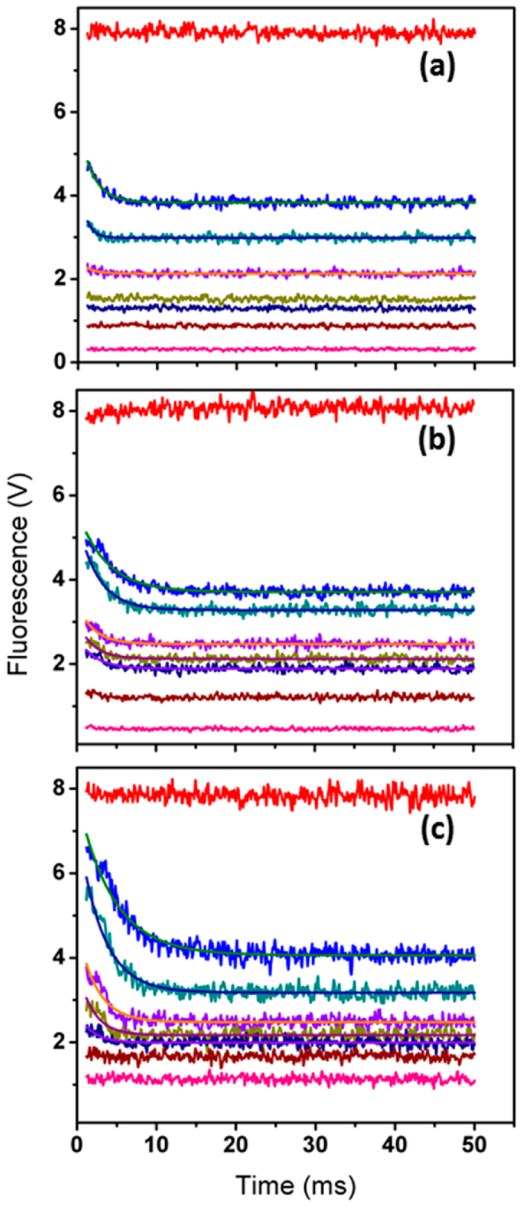

Figure 3. Stopped-flow kinetics data for 70 nM (a) hpU-QF, (b) hpPyA-QF, and (c) hpPy-QF RNA hairpins after mixing to form solutions containing final concentrations of 0 (red), 5 (blue), 10 (cyan), 25 (violet), 50 (gold), 100 (navy), and 500 (brown) mM KCl. The pink curves show the background fluorescence of the blank buffer solution.

that for hpU, which has only uracils. Uracils have little or no propensity to stack, whereas cystosine and adenosine prefer stacked arrangements. hpPy-QF and hpPyA-QF have comparable isomerization rates that are faster than hpU-QF. Since hpPy and hpPyA rates are so similar, we suggest the alternative base-pairing schemes predicted for these structures may not serve a prominent role in the folding kinetics of these hairpins. Instead, we are left with the loop composition as the main contributing element for rapid isomerization.

The amplitudes of the fast isomerization component, reflecting the fraction of molecules in the sample undergoing fast isomerization, are small for all salt concentrations and never exceed 20% (Figure 4c). This result is in contrast to DNA hairpin studies where large amplitudes were measured,[20] suggesting that the RNA hairpins studied here have a greater preference for their native conformations compared to that of the DNA hairpins studied previously.

Whereas the intermediate isomerization reactions probed by FCS reveal faster kinetics for the RNA hairpins with cytosine and adenine in the loop, the stopped-flow kinetics data reveals the opposite trend for the slow isomerization. As shown in Figure 5, the relaxation time for hpU-QF is below 2 ms in 5 mM KCl and falls below the mixing time for KCl concentrations above 25 mM. By contrast, both hpPy-QF and hpPyA-QF show relaxation times above or near 2 ms up to 100 mM KCl (see Supporting Information Table S6). Hence, the isomerization reaction probed by the stopped-flow experiment occurs much slower for the hairpins containing cytosine and adenine in the loop.

Results of Control Experiments and Mechanisms of Quenching. FCS experiments with the control DNA construct (ssTGdna-F) confirm that quenching is not simply a consequence of the increased salt concentration, since both the number of molecules and the brightness are constant (Figure 6a,b). Just as expected, ssTGdna-F does not exhibit meaningful isomerization times; instead, all data can be well-described by the model with the fast relaxing (≈4 μs) triplet state only.

The results obtained with the single-stranded doubly labeled RNA (ssU-QF) reveal the contribution of random encounters between TAMRA and dabcyl to quenching of fluorescence. This process is fast (it is not observed directly in either auto- or cross-correlations, data not shown) and hence does not influence the apparent number of molecules (Figure 6a). Brightness per molecule, however, is reduced (Figure 6b), indicating that quenching takes place and is more efficient at higher salt concentration. We conclude that quenching by random encounter is too fast (1 μs or faster) to be observed in our FCS experiment and hence it does not contribute to isomerization phases observed with the RNA hairpins.

The RNA hairpin without the quencher (hpU-F) exhibits a fast isomerization phase but shows no presence of a slow phase. As shown in Figure 6a, the number of molecules for hpU-F is constant for all KCl concentrations. Therefore, the slow phase observed in doubly labeled hairpins must be due to dabcyl-dependent quenching. The brightness per molecule of hpU-F remains nearly constant (Figure 6b), showing that closing of the hairpin has little effect on TAMRA fluorescence in the absence of the quencher. However, we observed a fast phase in the autocorrelations of hpU-F. We interpret this reaction as dynamics of the RNA chain, which results in TAMRA quenching by guanines. Notably, parameters of the fast isomerization reaction are different for hpU-F and hpU-QF (Figure 6c,d). It should be remembered that populations of observed molecules are very different in these two cases, and quenching by dabcyl certainly dominates detectable isomerization reactions. In all doubly labeled hairpins, autocorrelations decay much faster at high salt concentrations, an effect that is not observed with hpU-F.

The absolute values of molecular brightness are different for all four constructs shown in Figure 6b. One likely cause is quenching of the fluorophore by nucleotides, either through stacking or by collision. Guanosine in particular is known to quench fluorophores when they stack with it, such as in the ssTGdna-F construct. The ssU-QF RNA has no guanosines, and its molecular brightness is greatest, consistent with an absence of stacking by uridines. The observation that brightness in the hairpin is reproducibly higher in the presence of

DOI: 10.1021/bi5014276
Biochemistry 2015, 54, 1886−1896

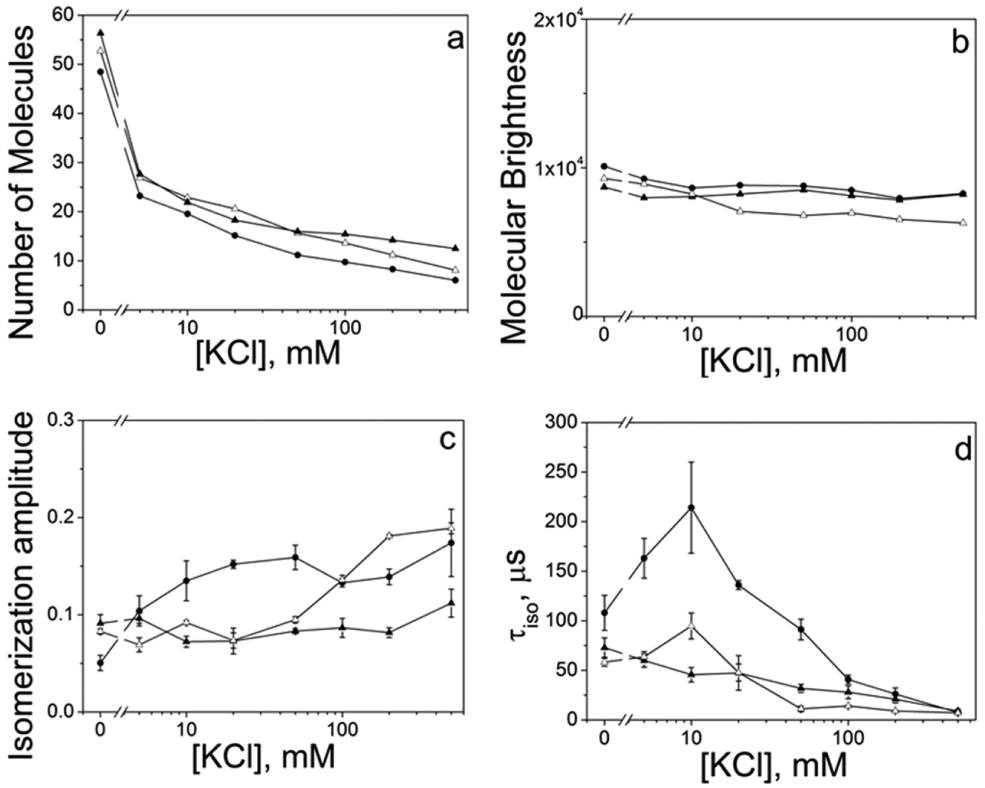

Figure 4. Results of FCS analysis of the doubly labeled hairpins with different loop composition as a function of KCl concentration: (a) number of molecules normalized by the average fluorescence, (b) brightness per molecule, (c) amplitude of the fast isomerization, and (d) time constant of the fast isomerization (●, hpU-QF; ▲, hpPy-QF; Δ, hpPyA-QF).

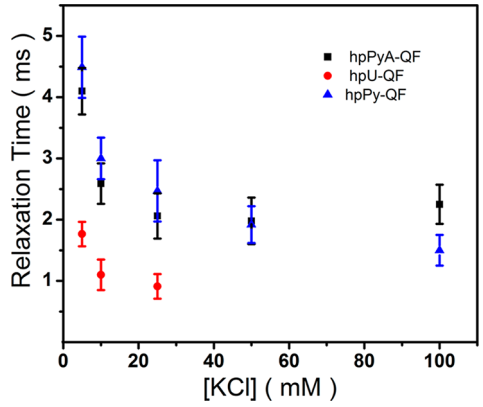

Figure 5. Relaxation times vs KCl concentration from single-exponential fits to the stopped kinetics data shown in Figure 3 (●, hpU-QF; ▲, hpPy-QF; ■, hpPyA-QF).

quencher (hpU-QF and hpU-F) seems somewhat anomalous; however, once the hairpin is folded, TAMRA fluorescence is fully quenched only in hpU-QF.

■ DISCUSSION

This investigation into the stability and folding dynamics for three RNA hairpins as a function of KCl concentration provides new information on the parameters that control folding. An important result of our studies is that folding in these hairpins is not a two-state process when viewed from the perspective of 5′−3′ end contact formation. The first piece of evidence that supports this conclusion comes from the fact that the melting temperature depends on the spectroscopic signal that is used to monitor unfolding. The results of FCS experiments lend further support to this interpretation. In all hairpins, we observe a dramatic reduction in the apparent number of molecules for increasing salt concentration. We attribute this loss to isomerization of the hairpins that is too slow to be observed by FCS directly, but it was observed in subsequent stopped-flow experiments. Therefore, there are two kinetic steps and at least three states in hairpin folding.

These results are in general agreement with earlier FCS studies by the same method[19,20] that found three populations in analogous DNA hairpins; one population was characterized by a slow isomerization time not directly accessible by FCS. This slow isomerization reaction was subsequently observed directly by stopped flow.[23] In a more recent FCS study, both the fast and slow isomerization reactions were observed in the same experiment using a new FCS technique termed diffusion-decelerated FCS.[22] While the results presented here are qualitatively very similar, the RNA hairpins display a broader range of relaxation times and smaller amplitudes for the faster isomerization.

What is the nature of the fast and slow isomerization phases in the RNA hairpins studied here, and why do the relaxation times for the hpPy-QF and hpPyA-QF hairpins appear to be faster in the FCS measurements and slower in the stopped-flow measurements compared to hpU-QF hairpins? While it is hard to draw conclusions about these processes based solely on the behavior of attached fluorescent dye and quencher groups, we have shown that these processes are dabcyl-dependent and hence must correspond to RNA chain dynamics that brings the dye and the quencher in direct contact. The fact there are no discernible differences in the behavior of hpPy-QF and hpPyA-QF suggests the presence of alternative intermediate states,

DOI: 10.1021/bi5014276
Biochemistry 2015, 54, 1886−1896

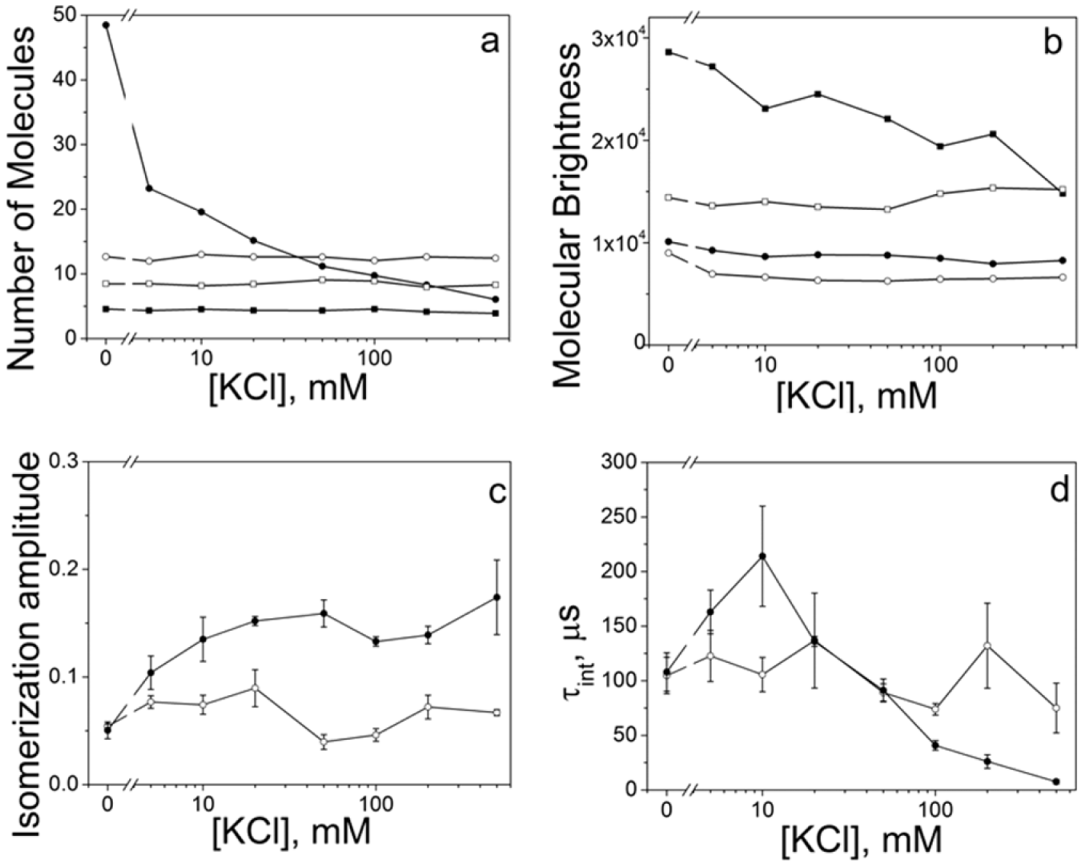

Figure 6. Comparison of the hairpin (hpU-QF) to the control samples: (a) number of molecules normalized by the average fluorescence, (b) brightness per molecule, (c) amplitude of the fast isomerization, and (d) time constant of the fast isomerization (●, hpU-QF; ○, hpU-F; ■, ssU-QF; □, ssTGdna-F).

such as those presented in Figures S1 and S2,[34] likely do not play a prominent role in the folding mechanism under the reaction conditions considered here. However, both sequences are thought to undergo base stacking in the loop region. Therefore, we hypothesize that base stacking in the loop of hpPy-QF and hpPyA-QF hairpins may be the dominant factor behind the observed differences.

The effect of stacking on DNA hairpin folding was investigated previously by Shen et al.[28] using laser-induced temperature jump and by Goddard et al.[27] and Wallace et al.[29] using FCS. These studies focused on short-stem DNA hairpins with large polyA loops in which base stacking was thought to be present. More recently, Mosayebi et al. examined similar DNA sequences using a coarse-grained molecular modeling approach to investigate stacking in the loop and its effect on the kinetics of loop closing.[30] In general, these studies considered the hairpin folding reaction as a two-state process and found stacking in the loop slows the loop closing kinetics relative to loop sequences with reduced propensity for stacking.

For the present study, we suggest the fast isomerization phases for all hairpins observed in our FCS experiments correspond to the reversible formation of a quenched or partially quenched intermediate state with a folded loop and a partially or incorrectly base-paired stem. The observed relaxation times, therefore, depend on the rates of folding and unfolding of the loop and formation and disruption of the base pairs in the stem. The time scale for these processes (~20−200 μs) is consistent with previous studies of DNA hairpins in which laser-induced temperature jump,[28,36] FCS,[10] and related techniques were used to observe relaxation times attributed to the formation of stable DNA hairpin loops.

The rate of the fast isomerization reaction is enhanced by the presence of cytosine and adenine in the loop. Relaxation times for hpU-QF ranged from ~100 to 200 μs, whereas faster relaxation times of ~20−70 μs were observed for hpPy-QF and hpPyA-QF. To further investigate this fast isomerization process of our RNA hairpins, we estimate the respective contributions from the forward and reverse reactions to the overall relaxation rate. The overall RNA folding reaction is represented by the reaction scheme

$$\mathrm{U} \underset{k_{-1}}{\overset{k_1}{\rightleftharpoons}} \mathrm{I} \underset{k_{-2}}{\overset{k_2}{\rightleftharpoons}} \mathrm{N} \qquad \text{(Scheme 1)}$$

Here, U represents RNA molecules in the unfolded state, I is a folded intermediate, and N is the native folded RNA. The reaction U ⇌ I is the fast isomerization reaction observed in our FCS experiments. The forward direction of this reaction represents loop closure and formation of the intermediate base pairs, and the reverse direction represents dissociation of the intermediate base pairs and loop opening. The relaxation time of the fast isomerization, τ_{iso}, is related to the forward and reverse rate constants, k_1 and k_{-1}, by the equation

$$\frac{1}{\tau_{iso}} = k_1 + k_{-1} \qquad (5)$$

Also, the equilibrium constant for the intermediate reaction is given by $K_{eq} = k_1/k_{-1}$. The contributions of the forward and

DOI: 10.1021/bi5014276
Biochemistry 2015, 54, 1886−1896

reverse reactions to τ_{iso} are thus obtained from K_{eq} and τ_{iso}. Assuming the intermediate state is nonfluorescent, we can estimate K_{eq} from the correlation amplitude using

$$K_{eq} = \frac{B}{1 - B} \quad (6)$$

As a representative example, we consider the FCS data for the three RNA hairpin samples in 20 mM KCl. Under these conditions, our FCS analysis of the fast isomerization reaction reveals τ_{iso} = 136, 47.4, and 47.8 μs and B = 0.152, 0.073, and 0.074 for hpU-QF, hpPy-QF, and hpPyA-QF, respectively (see Tables S4 and S5). From eq 6, we obtain K_{eq} = 0.18 for hpU-QF and K_{eq} = 0.079 for hpPy-QF and hpPyA-QF. Therefore, for hpU-QF, $k_1 = 1.1 \times 10^3$ s^{-1} and $k_{-1} = 6.2 \times 10^3$ s^{-1}. For hpPy-QF and hpPyA-QF, $k_1 = 1.5 \times 10^3$ s^{-1} and $k_{-1} = 1.9 \times 10^4$ s^{-1}. The closing rates (k_1) are similar for all three hairpins, whereas the opening rates (k_{-1}) are much faster for hpPy-QF and hpPyA-QF than that for hpU-QF. This difference in opening rates is the dominant factor influencing the observed changes in relaxation time with sequence in our study. Similar calculations lead to qualitatively similar conclusions for samples with KCl concentrations between 10 and 100 mM. The presence of cytosine and adenine in the hpPy-QF and hpPyA-QF hairpin loops enhances the formation rate of the intermediate state to a small extent and the intermediate opening rate to a much larger extent. The larger opening rates suggest the intermediate states of the hpPy-QF and hpPyA-QF hairpins are less stable than those of the hpU-QF hairpins. We hypothesize that because the hpPy-QF and hpPyA-QF loops may have a greater propensity for base stacking, this base stacking may exert a sort of tension on the base pairs of the hpPy-QF and hpPyA-QF intermediate states, thus destabilizing the intermediates and increasing their opening rate.

We attribute the slow isomerization phases observed in our stopped-flow experiments to the formation of the natively folded hairpins (state N in Scheme 1) with the correctly base-paired stems. Similar prolonged relaxation times for analogous DNA hairpins folding into their native conformations have been observed previously using such techniques as single molecule fluorescence,[37,38] optical trapping,[39,40] stopped flow,[23,24,41] and FCS.[22]

For the RNA hairpins studied here, there is a dramatic difference in the slow isomerization rates for hairpins hpPy-QF amd hpPyA-QF compared to that for hairpin hpU-QF, such that the former hairpins exhibit greatly prolonged relaxation times compared to the latter. Furthermore, there is an interesting inverse relationship between the relaxation times of the fast and slow isomerization phases wherein faster relaxation of the intermediate coincides with slower relaxation of the native hairpin structure and vise versa. To interpret these observations, we suggest formation of the intermediate states observed in our FCS experiments may enhance folding of the native structure because these intermediates occupy regions of the folding free energy landscape near transition states between unfolded conformations (state U) and native folded conformations (state N). This idea is consistent with the fact that the intermediate (state I) must correspond to a state in which the dye and quencher are in close proximity with terminal base pairs at or near their native contacts. Accordingly, the stability of these intermediates may be important in governing the rate at which the native structure can form. When the intermediate state is more stable, the RNA structure is held in a position close to the transition state for a longer time, increasing the probability that all the native base-pair contacts will form before the intermediate base pairs can dissociate. Intermediates with lower stability are more likely to denature to unfolded state U before the native contacts can form. As we have suggested previously, the hpPy-QF and hpPyA-QF hairpins exhibit lower stability of their intermediates, leading to shorter intermediate lifetimes for these hairpins. These shorter intermediate lifetimes, in turn, may prolong the formation of the native hairpin. In the case of hpU-QF hairpins, the intermediate is more stable, which could explain why relaxation of the native hairpin occurs more rapidly.

The above interpretation is consistent with statistical mechanics modeling of different RNA hairpin structures reported by Zhang et al.[12,13] While this modeling does not specifically address base stacking, it underscores the important role of reaction intermediates in the kinetics of RNA hairpin formation. According to this modeling, reaction intermediates can enhance or slow the rate of folding, depending on whether they contain incorrect, off-path base pairings or native, on-path base pairings. When the intermediates contain on-path base pairings, as we suggest is the case for our RNA hairpins, the more stable the intermediates, the more the folding rate is enhanced, consistent with the observations reported here. The main factors investigated in this modeling regarding their effects on intermediate stability include the temperature of the solution relative to the melting temperature of the hairpin and the salt concentration. The present study suggests the propensity for base stacking in single-stranded regions may be an additional factor that should be addressed in future modeling of RNA folding kinetics.

What is particularly interesting about these RNA hairpin experiments is that the differences in stacking propensity of these pyrimidine loop sequences might at first seem inconsequential. Since all loops contain a preponderance of uridines that do not stack with other bases, they might be expected to dominate the behavior of the hairpins. Clearly, however, the presence of the interspersed cytosines alters the loop properties. While a more dramatic demonstration of the contribution of stacking to hairpin folding may certainly be seen in a comparison of hpU and hpA molecules (analogous to the DNA hairpins[27−30]), our RNA sequences represent typical polypyrimidine tracts observed in gene regulation sites. Their different properties could be important for interactions with other RNAs and with proteins.

With the realization that folding in nucleic acid hairpins is not a two-state process comes the need for a broader range of experimental techniques and probes that monitor folding. One problem that arises from this fact is structural interpretation of the results. We observe a change in the rate of fast isomerization as a function of salt, but we do not know if we are monitoring the same process at all salt concentrations. It is possible that multiple isomerization events change their rates and move in or out of the FCS time window. FCS experiments are also limited in the kinds of probes that are used to elucidate structure, and they usually require two probes for measuring proximity. With the labeling scheme used here, end contacts are detected, but events in the loop and loop−stem interactions remain largely unnoticed. Certainly, the RNA hairpin folding problem will benefit from concerted application of different probes and techniques. These data are important for predictions of co-transcriptional RNA folding, where folding kinetics can determine the functional structure of the RNA.

DOI: 10.1021/bi5014276
Biochemistry 2015, 54, 1886−1896

■ ASSOCIATED CONTENT

Supporting Information

Two-dimensional structure diagrams showing various conformations of hpPy and hpPyA RNA hairpins (Figure S1); excitation spectra of hpU-QF RNA hairpins (Figure S2); melting curves of hpU-QF RNA hairpins (Figure S3); melting temperatures of hpU-QF RNA hairpins (Figure S4); FCS fitting parameters for all the RNA molecules studied (Tables S1−S5); and relaxation times for all RNA hairpins studied (Table S6). This material is available free of charge via the Internet at http://pubs.acs.org.

■ AUTHOR INFORMATION

Corresponding Authors

*(K.B.H.) Telephone: 314-362-4196. Fax: 314-362-7183. E-mail: kathleenhal@gmail.com.

*(A.V.O.) Telephone: 970-491-6286. Fax: 970-491-1801. E-mail: vanorden@mail.colostate.edu.

Present Address

[‖](R.K.N) Department of Chemistry, Boston University, Boston, Massachusetts 02215, United States.

Author Contributions

[§]A.V.M. and R.K.N. contributed equally to this work.

Funding

This work was supported by the U.S. National Institutes of Health through an American Recovery and Reinvestment Act supplement to Grant GM077231 (K.B.H.) and by the U.S. National Science Foundation, Grant 0920588 (A.V.O.).

Notes

The authors declare no competing financial interest.

■ ACKNOWLEDGMENTS

We thank Olve Peersen for experimental assistance and helpful discussions. We also thank Grace Campagnola for technical assistance.

■ ABBREVIATIONS

FCS, fluorescence correlation spectroscopy; dabcyl, 4-(dimethyl amino azo)benzene-4-carboxylic acid

■ REFERENCES

(1) Bevilacqua, P. C., and Blose, J. M. (2008) Structure, kinetics, thermodynamics, and biological functions of RNA hairpins. *Annu. Rev. Phys. Chem. 59*, 79−103.

(2) Stancik, A. L., and Brauns, E. B. (2008) Rearrangement of partially ordered stacked conformations constributes to the rugged energy landscape of small RNA hairpins. *Biochemistry 47*, 10834−10840.

(3) Sarkar, K., Meister, K., Sethi, A., and Gruebele, M. (2009) Fast folding of an RNA tetraloop on a rugged energy landscape detected by a stacking sensitive probe. *Biophys. J. 97*, 1418−1427.

(4) Zhang, W., and Chen, S.-J. (2002) RNA hairpin folding kinetics. *Proc. Natl. Acad. Sci. U.S.A. 99*, 1931−1936.

(5) Hyeon, C., and Thirumalai, D. (2008) Multiple probes are required to explore and control the rugged energy landscape of RNA hairpins. *J. Am. Chem. Soc. 130*, 1538−1539.

(6) Riccardi, L., Nguyen, P. H., and Stock, G. (2009) Free-energy landscape of RNA hairpins constructed via dihedral angle principal component analysis. *J. Phys. Chem. B 113*, 16660−16668.

(7) Xia, T., Santa Lucia, J., Jr., Burkard, M., Kierzek, R., Schroeder, S. J., Jaio, X., Cox, C., and Turner, D. H. (1998) Thermodynamics parameters for an expanded nearest-neighbor model for formation of RNA duplexes with Watson−Crick base pairs. *Biochemistry 37*, 14719−14735.

(8) Mathews, D. H., Sabina, J., Zuker, M., and Turner, D. H. (1999) Expanded sequence dependence of thermodynamics parameters improves predictions of RNA secondary structure. *J. Mol. Biol. 288*, 911−940.

(9) Kuznetsov, S. V., Ren, C.-C., Woodson, S., and Ansari, A. (2008) Loop dependence of the stability and dynamics of nucleic acid hairpins. *Nucleic Acids Res. 36*, 1098−1112.

(10) Bonnet, G., Krichevsky, O., and Libchaber, A. (1998) Kinetic conformational fluctuations of nucleic acid hairpins. *Proc. Natl. Acad. Sci. U.S.A. 95*, 8602−8606.

(11) Chen, S.-J., and Dill, K. A. (2000) RNA folding energy landscape. *Proc. Natl. Acad. Sci. U.S.A. 97*, 646−651.

(12) Zhang, W., and Chen, S.-J. (2006) Exploring the complex folding kinetics of RNA hairpins: I. General folding kinetics analysis. *Biophys. J. 90*, 765−777.

(13) Zhang, W., and Chen, S.-J. (2006) Exploring the complex folding kinetics of RNA hairpins: II. Effect of sequence, length, and misfolded states. *Biophys. J. 90*, 778−787.

(14) Flamm, C., Fontana, W., Hofacker, I. L., and Schuster, P. (2000) RNA folding elementary step resolution. *RNA 6*, 325−338.

(15) Lin, M. M., Meinhold, L., Shorokhov, D., and Zewail, A. H. (2008) Unfolding and melting of DNA (RNA) hairpins: the concept of structure specific 2D dynamics landscapes. *Phys. Chem. Chem. Phys. 10*, 4227−4239.

(16) Bowman, G. R., Huang, X., Yao, Y., Sun, J., Carlsson, G., Guibas, L. J., and Pande, V. S. (2008) Structural insight into RNA hairpin folding intermediates. *J. Am. Chem. Soc. 130*, 9676−9678.

(17) Portella, G., and Orozco, M. (2010) Multiple routes to characterize the folding of small DNA hairpin. *Angew. Chem., Int. Ed. 49*, 7673−7676.

(18) Ma, H., Proctor, D. J., Kierzek, E., Kierzek, R., Bevilacqua, P. C., and Gruebele, M. (2006) Exploring the energy landscape of a small RNA hairpin. *J. Am. Chem. Soc. 128*, 1523−1530.

(19) Jung, J., Ihly, R., Scott, E., Yu, M., and Van Orden, A. (2008) Probing the complete folding trajectory of a DNA hairpin using dual beam fluorescence fluctuation spectroscopy. *J. Phys. Chem. B 112*, 127−133.

(20) Jung, J., and Van Orden, A. (2006) A three-state mechanism for DNA hairpin folding characterized by multiparameter fluorescence fluctuation spectroscopy. *J. Am. Chem. Soc. 128*, 1240−1249.

(21) Van Orden, A., and Jung, J. (2008) Fluroescence correlation spectroscopy for probing the kinetics and mechanisms of DNA hairpin formation. *Biopolymers 89*, 1−16.

(22) Yin, Y., Wang, P., Yang, X.-X., Li, X., He, C., and Zhao, X.-S. (2012) Panorama of DNA hairpin folding observed via diffusion-decelerated fluorescence correlation spectroscopy. *Chem. Commun. 48*, 7413−7415.

(23) Nayak, R. K., Peerson, O. B., Hall, K. B., and Van Orden, A. (2012) Millisecond time-scale folding and unfolding of DNA hairpins using rapid-mixing stopped-flow kinetics. *J. Am. Chem. Soc. 134*, 2453−2456.

(24) Narayanan, R., Zhu, L., Velmurugu, Y., Roca, J., Kuznetsov, S. V., Prehna, G., Lapidus, L. J., and Ansari, A. (2012) Exploring the energy landscape of nucleic acid hairpins using laser temperature-jump and microfluidic mixing. *J. Am. Chem. Soc. 134*, 18952−18963.

(25) Turner, D. H. (2000) Conformational changes, in *Nucleic Acids: Structures, Properties, and Functions* (Bloomfield, V. A., Crothers, D. M., and Tinoco, I., Jr., Eds.) pp 259−334, University Science Books, Sausalito, CA.

(26) Aalberts, D. P., Parman, J. M., and Goddard, N. L. (2003) Single-strand stacking free energy from DNA beacon kinetics. *Biophys. J. 84*, 3212−3217.

(27) Goddard, N. L., Bonnet, G., Krichevsky, O., and Libchaber, A. (2000) Sequence dependent rigidity of single stranded DNA. *Phys. Rev. Lett. 85*, 2400−2403.

DOI: 10.1021/bi5014276
Biochemistry 2015, 54, 1886−1896

(28) Shen, Y., Kuznetsov, S. V., and Ansari, A. (2001) Loop dependence of the dynamics of DNA hairpins. *J. Phys. Chem. B 105*, 12202−12211.
(29) Wallace, M. I., Ying, L., Balasubramanian, S., and Klenerman, D. (2001) Non-Arrhenius kinetics for the loop closure of a DNA hairpin. *Proc. Natl. Acad. Sci. U.S.A. 98*, 5584−5589.
(30) Mosayebi, M., Romano, F., Ouldridge, T. E., Louis, A. A., and Doye, J. P. K. (2014) The role of loop stacking in the dynamics of DNA hairpin formation. *J. Phys. Chem. B 118*, 14326−14335.
(31) Tyagi, S., Bratu, D. P., and Kramer, F. R. (1998) Multicolor molecular beacons for allele discrimination. *Nat. Biotechnol. 16*, 49−53.
(32) Elson, E. L., and Magde, D. (1974) Fluorescence correlation spectroscopy I. Conceptual basis and theory. *Biopolymers 13*, 1−27.
(33) Jung, J., and Van Orden, A. (2005) Folding and unfolding kinetics of DNA hairpins in flowing solutions by multiparameter fluorescence correlation spectroscopy. *J. Phys. Chem. B 109*, 3648−3657.
(34) Markham, N. R., and Zuker, M. (2008) UNAFold: software for nucleic acid folding and hybridization. *Methods Mol. Biol. 453*, 3−31.
(35) Xu, D., Evans, K. O., and Nordlund, T. M. (1994) Melting and premelting transitions of an oligomer measured by DNA base fluorescence and absorption. *Biochemistry 33*, 9592−9599.
(36) Ansari, A., Kuznetsov, S. V., and Shen, Y. (2001) Configuration diffusion down a folding funnel describes the dynamics of DNA hairpins. *Proc. Natl. Acad. Sci. U.S.A. 98*, 7771−7776.
(37) Grunwell, J. R., Glass, J. L., Lacoste, T. D., Deniz, A. A., Chemla, D. S., and Schultz, P. G. (2001) Monitoring the conformational fluctuations of DNA hairpins using single pair fluorescence resonance energy transfer. *J. Am. Chem. Soc. 123*, 4295−4303.
(38) Tsukanov, R., Tomov, T. E., Masoud, R., Drory, H., Plavner, N., Liber, M., and Nir, E. (2013) Detailed study of DNA hairpin dynamics using single-molecule fluorescence assisted by DNA origami. *J. Phys. Chem. B 117*, 11932−11942.
(39) Woodside, M. T., Anthony, P. C., Behnke-Parks, W. M., Larizadeh, K., Herschlag, D., and Block, S. M. (2006) Direct measurement of the full sequence-dependent folding landscape of a nucleic acid. *Science 314*, 1001−1004.
(40) Woodside, M. T., Behnke-Parks, W. M., Larizadeh, K., Travers, K., Herschlag, D., and Block, S. M. (2006) Nanomechanical measurements of the sequence-dependent folding landscapes of single nucleic acid hairpins. *Proc. Natl. Acad. Sci. U.S.A. 103*, 6190−6195.
(41) Nayak, R. K., and Van Orden, A. (2013) Counterion and polythymidine loop-length dependent folding and thermodynamic stability of DNA hairpins reveal the unusual counterion-dependent stability of tetraloop hairpins. *J. Phys. Chem. B 117*, 13956−13966.

DOI: 10.1021/bi5014276
Biochemistry 2015, 54, 1886−1896